



# A Numerical Study on Determining the Effect of Original Evaporator Design on DX-SAHP System Performance

Rıdvan Yakut<sup>1\*</sup>

<sup>1\*</sup> Kafkas University, Faculty of Engineering and Architecture, Department of Mechanical Engineering, Kars, Turkey, (ORCID: 0000-0002-4145-7280),  
[ryakut@kafkas.edu.tr](mailto:ryakut@kafkas.edu.tr)

(1st International Conference on Applied Engineering and Natural Sciences ICAENS 2021, November 1-3, 2021)

(DOI: 10.31590/ejosat.1012486)

**ATIF/REFERENCE:** Yakut, R. (2021). A Numerical Study on Determining the Effect of Original Evaporator Design on DX-SAHP System Performance. *European Journal of Science and Technology*, (28), 1052-1055.

## Abstract

Greenhouse gases caused by non-renewable energy sources bring about global warming and climate change. Therefore, renewable energy sources, which are clean, economical and unlimited energy sources, come to the fore. In the numerical study carried out, a unique finned evaporator design was made to increase the efficiency of the integrated direct expansion solar-assisted heat pump systems (DX-SAHP). In the numerical analysis carried out in the ANSYS Fluent program, it was determined that the COP and electrical efficiency of the system were in good agreement with the results in the literature. As a result of the numerical analysis, COP was obtained as 3.88 and 3.60 for 0.025 kg/s and 0.050 kg/s flow rates, respectively. It was also determined that the electrical efficiency increased by 12% compared to natural convection in both flow rates.

**Keywords:** DX-SAHP, renewable energy, heat pump, evaporator design, numerical analysis.

## Orijinal Evaporatör Tasarımının DX-SAHP Sistem Performansına Etkisinin Belirlenmesi Üzerine Sayısal Bir Çalışma

### Öz

Yenilenemeyen enerji kaynaklarının neden olduğu sera gazları küresel ısınmaya ve iklim değişikliğine neden olmaktadır. Bu nedenle temiz, ekonomik ve sınırsız enerji kaynağı olan yenilenebilir enerji kaynakları ön plana çıkmaktadır. Gerçekleştirilen sayısal çalışmada, entegre doğrudan genişlemeli güneş destekli ısı pompası sistemlerinin (DX-SAHP) verimliliğini artırmak için benzersiz bir kanatlı evaporatör tasarımı yapılmıştır. ANSYS Fluent programında yapılan sayısal analizde sistemin COP ve elektriksel veriminin literatürdeki sonuçlarla iyi bir uyum içinde olduğu tespit edilmiştir. Sayısal analiz sonucunda 0,025 kg/s ve 0,050 kg/s debiler için COP sırasıyla 3,88 ve 3,60 olarak elde edilmiştir. Ayrıca her iki akış hızında da elektriksel verimin doğal konveksiyona göre %12 arttığı tespit edilmiştir.

**Anahtar Kelimeler:** DX-SAHP, yenilenebilir enerji, ısı pompası, evaporatör tasarımı, nümerik analiz.

\* Corresponding Author: [ryakut@kafkas.edu.tr](mailto:ryakut@kafkas.edu.tr)

## 1. Introduction

World population and energy consumption are increased by more than 10% in the last 10 years. Due to increasing energy requirement, mankind has turned to unlimited energy sources such as renewable energy from limited energy sources such as fossil and nuclear energy. The most preferred method among renewable energy sources is energy production with solar energy. According to the International Renewable Energy Agency data, photovoltaic (PV) systems constitute 98.7% of the electrical energy produced by solar sources (Irena, 2018). Therefore, the efficiency of solar energy generation is directly related to the efficiency of PV cells. PV systems provide clean, environmentally friendly, economical and unlimited energy production by converting the energy from the sun directly into energy.

However, cells made of different materials radiate at different wavelengths depending on the characteristics of the material which they are produced and turn into electrical energy (Kandilli, Külahlı, & Savcı, 2013). Solar radiation needs energy in the range of 0 to 1.12 eV in order to generate voltage by removing electrons from the photovoltaic cell (Masters, 2004). In Figure 1, the variation of the energy required to remove electrons with photons with wavelength is given. If the energy of the photon is above this range, it will be stored as heat in the system and cause the system efficiency to decrease (Cuce & Riffat, 2017; Ömeroğlu, 2018b).

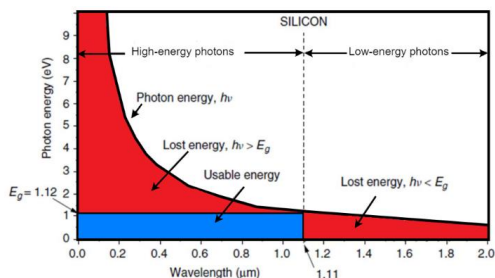


Figure 1. Wavelength and band gap energy (Masters, 2004)

PV-T systems are designed to convert solar energy more efficiently produce both heat and electricity at the same time. Although PV-T systems are successful systems in energy and heat production, many parameters, especially design, operation and climate parameters, affect the performance of PV-T systems (Abdullah, Misha, Tamaldin, Rosli, & Sachit, 2019). Although the design and operation parameters can be calculated numerically and optimum conditions can be determined, since climatic parameters such as solar radiation, relative humidity, wind velocity, ambient temperature, and accumulated dust change constantly depending on ambient conditions, it is not possible to determine them numerically (Abdullah et al., 2019). In addition, the long-term decrease in the efficiency of solar cells that are constantly exposed to solar radiation makes it difficult to determine the performance of solar energy systems numerically (Chegaar, Ouennoughi, & Guechi, 2004; Cuce & Cuce, 2014; Cuce, Cuce, & Bali, 2013; Du, Hu, & Kolhe, 2012). Therefore, these parameters should be taken into account when determining the amortization periods of PV-T systems (Ozakin, Yakut, & Khalaji, 2020). Although the determination of PV-T system efficiency by numerical analysis involves uncertainties, numerical analysis is the most effective method in determining the performance of different designs quickly, economically and easily. Computational fluid dynamics (CFD) is important in determining the effect of basic design and operating parameters on system performance with high accuracy (Kalkan, Ezan, Duquette, Yilmaz Balaman, & Yilanci, 2019)

In the present study, the efficiency coefficient (COP) and electrical efficiency of the photovoltaic evaporator with the original channel design in the photovoltaic thermal solar-assisted heat pump (PVT-SAHP) system were determined using the ANSYS Fluent program.

## 2. Material and Method

### 2.1. PVT-SAHP System

The PV-SAHP system operates on the principle of using the heat drawn from the photovoltaic system as source heat in the heat pump. The schematic representation of the PVT-SAHP system is shown in Figure 2. PVT-SAHP cooling systems generally consist of PV panel used as evaporator, compressor, condenser, and expansion valve. SAHP has two types as direct expansion SAHP (DXSAHP) and indirect expansion SAHP (IDX-SAHP) according to the connection type of solar collector and heat pump evaporator (Wang, Guo, Zhang, Yang, & Mei, 2017). In the present study simulation is based on DXSAHP system.

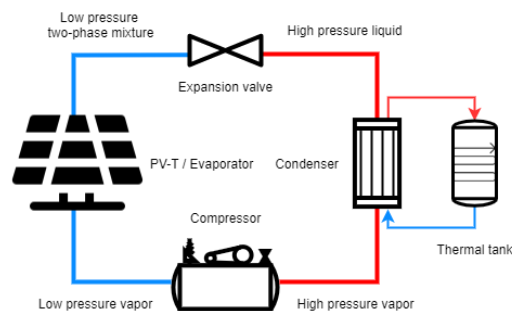


Figure 2. Schematic representation of the DXSAHP system.

The numerical study was carried out for 1600×1000 mm evaporator size, solar radiation of 1000 W/m<sup>2</sup>. At this intensity of radiation, the cell temperature is approximately 85 °C. The variation of the electrical efficiency against the temperature values reached by the photovoltaic cells in the uncooled state is given in Figure 3.

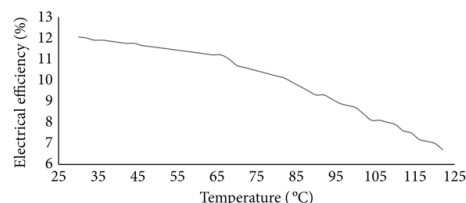


Figure 3. The electrical efficiency of uncooled PV cells by temperature (Ömeroğlu, 2018a).

Ozakin created the COP – evaporation temperature graph based on the values in the literature (Ozakin et al., 2020). In the study, COP values were calculated based on the graph in Figure 4.

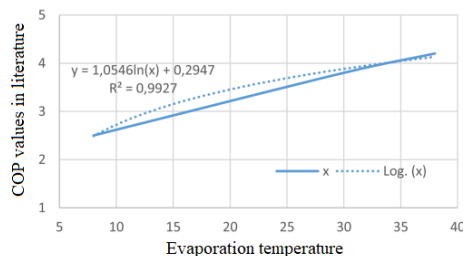


Figure 4. Variation of COP values in the literature versus evaporation temperature (Ozakin et al., 2020).

### 2.2. Numerical Model

The numerical model of the DX-SAHP system, in which the COP and electrical efficiency are calculated, is given in Figure 5.

a. b.

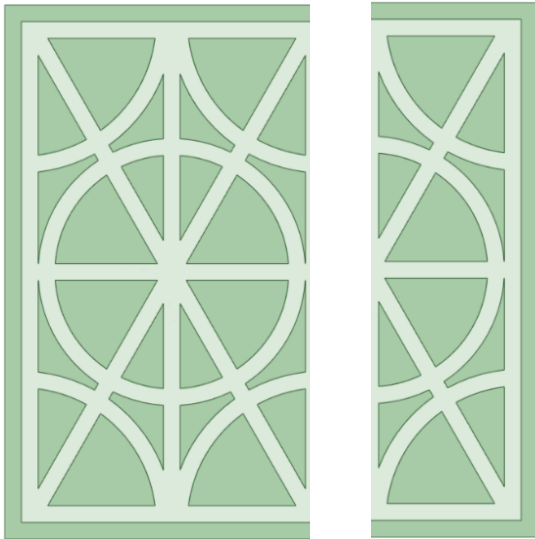


Figure 5. a. Numerical micro-channel model, b. symmetry model

The water is at 1 atm pressure and 293K conditions at the heat pump inlet, flows through the originally designed micro-channel and removes the heat from the photovoltaic system. The boundary conditions of the numerical model are given in Table 1.

Table 1. Boundary conditions

| Model               | Symmetry              |
|---------------------|-----------------------|
| Fluid               | Water                 |
| Heat Flux           | 1000 W/m <sup>2</sup> |
| Inlet               | 0.025 – 0.050 kg/s    |
| Outlet              | Pressure Outlet       |
| Other Surfaces      | Wall                  |
| Number of Iteration | 200                   |
| Number of Mesh      | 466346                |

The designed micro-channel is suitable for symmetric modeling; therefore, the symmetric model was used in the analysis. Thus, both analyzes were solved in a shorter time and more meshes were created on the model. The analyzes were calculated to converge at 250 iterations.

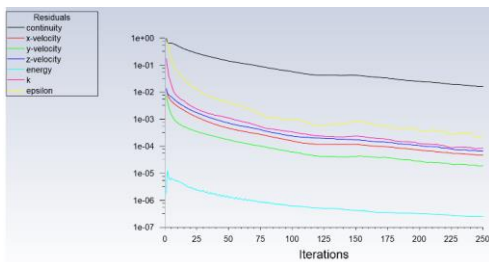


Figure 6 . Scaled residuals

Mesh parameters are important for obtaining accurate results in numerical analysis. A good mesh provides convergence of the problem. Although the mesh quality increases as the mesh number increases, generating more mesh than the optimum mesh number has no effect on the results and increases the solution time. Therefore, it is necessary to determine the optimum mesh number in the analysis. Although mesh metric contains many parameters, the three most important parameters are aspect ration, skewness and orthogonal quality. In numerical analysis, it is not desired that the aspect ratio value be higher than 30, and the smaller it is, the more accurate results are obtained. Another important mesh parameter, the skewness value should be close to 0, and the orthogonal quality should be close to 1.

Skewness mesh metrics spectrum:

| Excellent | Very good | Good      | Acceptable | Bad       | Unacceptable |
|-----------|-----------|-----------|------------|-----------|--------------|
| 0-0.25    | 0.25-0.50 | 0.50-0.80 | 0.80-0.94  | 0.95-0.97 | 0.98-1.00    |

Orthogonal Quality mesh metrics spectrum:

| Unacceptable | Bad        | Acceptable | Good      | Very good | Excellent |
|--------------|------------|------------|-----------|-----------|-----------|
| 0-0.001      | 0.001-0.14 | 0.15-0.20  | 0.20-0.69 | 0.70-0.95 | 0.95-1.00 |

Figure 7. Skewness and orthogonal quality spectrums (Matsson, 2021).

As a result of the mesh independence analysis are given in Figure 8. The optimum mesh number was determined as approximately 750,000 and the studies were carried out on this mesh number.

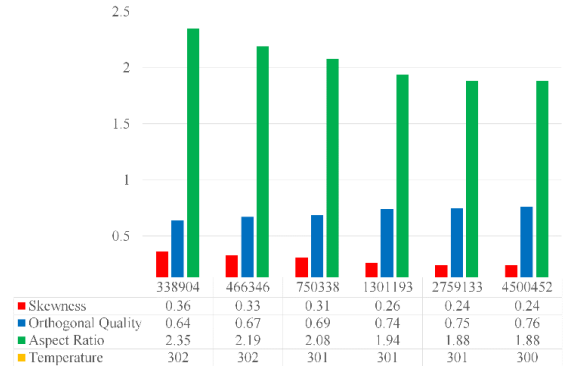


Figure 8. Mesh independence analysis results

### 2.3. Governing Equations

Three-dimensional continuity, turbulent energy, and turbulent momentum equations are solved with ANSYS Fluent under the appropriate boundary condition. The conservation equations for turbulent flow in cartesian coordinates are written as follows [7-8].

Continuity equation

$$\frac{\partial \rho \bar{u}_i}{\partial x_i} = 0 \quad (1)$$

The governing equation for solid

$$\frac{\partial}{\partial x_i} \left( k_s \frac{\partial T}{\partial x_i} \right) = 0 \quad (2)$$

Momentum equation

$$\rho \bar{u}_j \frac{\partial \bar{u}_i}{\partial x_j} = - \frac{\partial \bar{p}}{\partial x_i} + \frac{\partial}{\partial x_j} \left[ \mu_t \left( \frac{\partial \bar{u}_i}{\partial x_j} + \frac{\partial \bar{u}_j}{\partial x_i} \right) \right] \quad (3)$$

Energy equation

$$\rho \bar{u}_j \frac{\partial \bar{T}}{\partial x_j} = - \frac{\partial}{\partial x_j} \left[ \left( \frac{\mu_l}{\sigma_l} + \frac{\mu_t}{\sigma_t} \right) \frac{\partial \bar{T}}{\partial x_j} \right] \quad (4)$$

Transport equation for k

$$\rho \bar{u}_j \frac{\partial k}{\partial x_j} = \frac{\partial}{\partial x_j} \left( \frac{\mu_t}{\sigma_k} \frac{\partial k}{\partial x_j} \right) + \mu_t \left( \frac{\partial \bar{u}_i}{\partial x_j} + \frac{\partial \bar{u}_j}{\partial x_i} \right) \frac{\partial \bar{u}_i}{\partial x_j} - \rho \epsilon \quad (5)$$

Transport equaiton for ε

$$\rho \bar{u}_j \frac{\partial \varepsilon}{\partial x_j} = \frac{\partial}{\partial x_j} \left( \mu_t \frac{\partial \varepsilon}{\partial x_j} \right) + C_1 \mu_t \frac{\varepsilon}{k} \left( \frac{\partial \bar{u}_i}{\partial x_j} + \frac{\partial \bar{u}_j}{\partial x_i} \right) \frac{\partial \bar{u}_i}{\partial x_j} - C_2 \rho \frac{\varepsilon^2}{k} \quad (6)$$

The values of the empirical constants in the equation are given below

$$\sigma_k = 1.0, \sigma_\varepsilon = 1.3, C_\mu = 0.09, C_1 = 1.44, C_2 = 1.92$$

### 3. Results and Discussion

The temperature contours are given in Figure 9. It was observed that the surface temperature in the inlet region was low in both flow rates. In both flow rates, it was observed that heat transfer improved as turbulence intensity increased with the flow rate in the inlet region. However, since the temperature of the fluid increases towards the channel outlet, it has been observed that the surface temperature is high even where the flow rate is relatively high. Especially at 0.025 kg/s flow rate, although there are channels with high flow velocity in the bottom right corner of the channel, it has been observed that the surface temperatures are high. As a result of the analysis, the average surface temperatures were calculated as 301 K for 0.025 kg/s and 298 K for 0.050 kg/s.

Stream lines obtained in the designed microchannel are given in Figure 10. It has been observed that the flow was stationary in some places in the channel. Flow velocity increased even more in narrow sections. In addition, the flow rate in the horizontal channels were almost stationary in both flow rates. As a result of the analysis, average flow velocities were calculated as 0.017 m/s for 0.025 kg/s flow and 0.033 m/s for 0.050 kg/s.

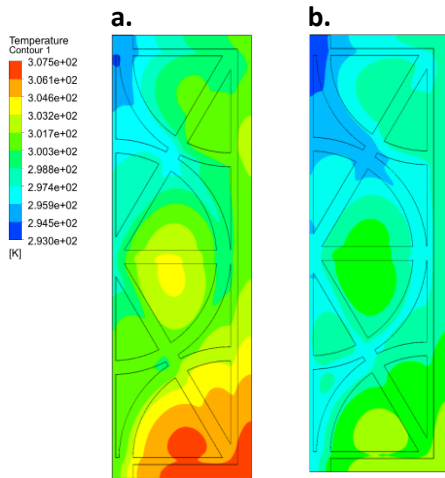


Figure 11. Temperature contours for a. 0.025 kg/s, b. 0.050 kg/s flow rates.

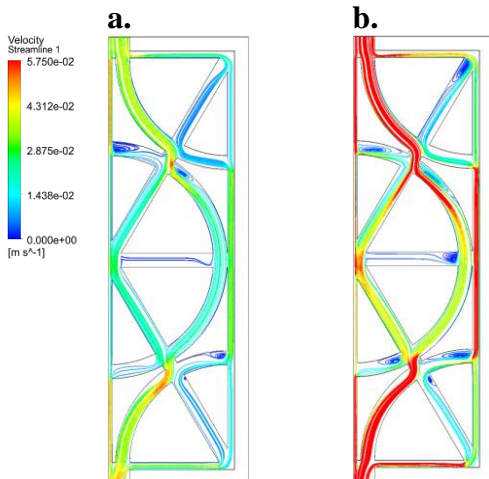


Figure 12. Velocity stream lines for a. 0.025 kg/s, b. 0.050 kg/s flow rates.

### 4. Conclusions and Recommendations

Average surface temperatures and average flow rates were determined for the DXSAHP system. The increase in electrical efficiency and COP values are given in Table 2.

Table 2. COP and electrical efficiency results

| Flow rate  | COP  | Electrical efficiency |
|------------|------|-----------------------|
| 0.025 kg/s | 3.88 | ~%12                  |
| 0.050 kg/s | 3.60 | ~%12                  |

As a result of the analysis, it was determined that cooling the DXSAHP system with an originally designed microchannel increases the electrical efficiency by approximately 12% in both flow rates. In addition, the COP was obtained as 3.88 at low flow rate and 3.60 at high flow rate.

### References

Abdullah, A. L., Misha, S., Tamaldin, N., Rosli, M. A. M., & Sachit, F. A. (2019). A Review: Parameters affecting the PVT collector performance on the thermal, electrical, and overall efficiency of PVT system. *Journal of Advanced Research in Fluid Mechanics and Thermal Sciences*, 60(2), 191-232.

Chegaar, M., Ouennoughi, Z., & Guechi, F. (2004). Extracting dc parameters of solar cells under illumination. *Vacuum*, 75(4), 367-372.

Cuce, E., & Cuce, P. M. (2014). Improving thermodynamic performance parameters of silicon photovoltaic cells via air cooling. *International Journal of Ambient Energy*, 35(4), 193-199.

Cuce, E., Cuce, P. M., & Bali, T. (2013). An experimental analysis of illumination intensity and temperature dependency of photovoltaic cell parameters. *Applied Energy*, 111, 374-382.

Cuce, E., & Riffat, S. B. (2017). A smart building material for low/zero carbon applications: heat insulation solar glass—characteristic results from laboratory and in situ tests. *International Journal of Low-Carbon Technologies*, 12(2), 126-135.

Du, B., Hu, E., & Kolhe, M. (2012). Performance analysis of water cooled concentrated photovoltaic (CPV) system. *Renewable and sustainable energy reviews*, 16(9), 6732-6736.

Irena, R. C. S. (2018). International Renewable Energy Agency (IRENA). *Abu Dhabi, UAE*.

Kalkan, C., Ezan, M. A., Duquette, J., Yilmaz Balaman, Ş., & Yilanci, A. (2019). Numerical study on photovoltaic/thermal systems with extended surfaces. *International Journal of Energy Research*, 43(10), 5213-5229.

Kandilli, C., Külahlı, G., & Savcı, G. (2013). Fotovoltaik Termal (PVT) Sistem 2D Termodinamik Modellenmesi ve Deneysel Sonuçlarla Karşılaştırılması, 11. *Ulusal Tesisat Mühendisliği Kongresi*, 17, 20.

Masters, G. M. (2004). Photovoltaic materials and electrical characteristics.

Matsson, J. E. (2021). *An Introduction to ANSYS Fluent 2021*: SDC Publications.

Ozakin, A. N., Yakut, K., & Khalaji, M. N. (2020). Performance analysis of photovoltaic-heat pump (PV/T) combined systems: A comparative numerical study. *Journal of Solar Energy Engineering*, 142(2).

Ömeroğlu, G. (2018a). CFD analysis and electrical efficiency improvement of a hybrid PV/T panel cooled by forced air circulation. *International Journal of Photoenergy*, 2018.

Ömeroğlu, G. (2018b). Fotovoltaik-Termal (PV/T) Sistemin Sayısal (CFD) ve Deneysel Analizi. *Fırat Üniversitesi Mühendislik Bilimleri Dergisi*, 30(1), 161-167.

Wang, Z., Guo, P., Zhang, H., Yang, W., & Mei, S. (2017). Comprehensive review on the development of SAHP for domestic hot water. *Renewable and sustainable energy reviews*, 72, 871-881.